Inorganica Chimica Acta 476 (2018) 129–135

Contents lists available at ScienceDirect

Inorganica Chimica Acta

journal homepage: www.elsevier.com/locate/ica

Research paper

Synthesis, crystal structures and high-temperature spin-crossover of new inclusion compounds of iron(II) *tris*(pyrazol-1-yl)methane complex with *p*-sulfonatocalix[4]arene

Olga Shakirova [a], Natalia Kuratieva [b,c], Evgeniy Korotaev [b], Lyudmila Lavrenova [b,c], Alexander Ovsyannikov [d], Igor Antipin [d], Svetlana Solovieva [d,*]

[a] Komsomolsk-on-Amur State University, Lenin av. 27, Komsomolsk-on-Amur 681013, Russia
[b] A.V. Nikolaev Institute of Inorganic Chemistry, Siberian Division, Russian Academy of Sciences, Akad. Lavrentiev ave. 3, Novosibirsk 630090, Russia
[c] Novosibirsk State University, Pirogov str. 2, Novosibirsk 630090, Russia
[d] A.E. Arbuzov Institute of Organic and Physical Chemistry, Kazan Scientific Centre of the Russian Academy of Sciences, Arbuzov str. 8, Kazan 420088, Russia

ARTICLE INFO

Article history:
Received 10 November 2017
Received in revised form 22 January 2018
Accepted 17 February 2018
Available online 23 February 2018

Keywords:
Synthesis
Fe(II) complex
Tris(pyrazol-1-yl)methane
Calix[4]arene
Magnetochemistry
Spectroscopy

ABSTRACT

Novel inclusion compounds based on iron(II) *tris*(pyrazol-1-yl)methane $[Fe\{HC(pz)_3\}_2]^{2+}$ cation and *p*-sulfonatocalix[4]arene (C[4]AS) as a counterion of formulas $[Fe\{HC(pz)_3\}_2]_2(C[4]AS)\cdot 24H_2O$ (**II**) and $[Fe\{HC(pz)_3\}_2]_5(C[4]AS)_2\cdot 62H_2O$ (**III**) have been synthesized in the solid state and studied by SC-XDR. The inclusion of $[Fe\{HC(pz)_3\}_2]^{2+}$ cation into the macrocycle cavity with 1:1 host-guest stoichiometry in both cases was found. The magnetochemical investigation (μ_{eff}) of the dehydrated complex **I** of formula $[Fe\{HC(pz)_3\}_2]_5(C[4]AS)_2$ in the 78–500 K temperature range has shown a high-temperature $^1A_1 \Leftrightarrow {}^5T_2$ spin crossover (SCO) which was accompanied by thermochromism. The crossover temperature values for heating ($T_c\uparrow$) and cooling ($T_c\downarrow$) are equal to 390 K and 380 K, respectively.

1. Introduction

The coordination compounds of iron(II) with octahedral coordination structure of the FeN_6 core can exist in the two spin states such as a low-spin state (S = 0, $^1A_1$) and high-spin state (S = 2, $^5T_2$). The changing the spin multiplicity (spin crossover, SCO) occurs under different external stimuli: temperature, pressure or light irradiation [1–5]. In many cases, the SCO is accompanied by thermochromism (color change pink (magenta) ⇔ white). Such compounds are of interest as promising materials for the development of molecular electronics [6,7]. *Tris*(pyrazol-1-yl)methane (HC(pz)$_3$) is perspective nitrogen-containing tripodal neutral ligand for the synthesis of bistable complexes of Fe(II) [5]. It can stabilize a great variety of coordination motifs; among these, a facial chelate coordination with local C3 symmetry represents the most common coordination motif. In the cases of Fe(II) the bifacial wrapping of the metal with the formation of the coordination polyhedron FeN_6 is observed (Scheme 1). It creates prerequisites for the realization of spin crossover in this compound.

A series of iron(II) complexes of HC(pz)$_3$ with various counterions $[Fe\{HC(pz)_3\}_2]A_n\cdot mH_2O$ (A = Cl^-, Br^-, I^-, SiF_6^{2-}, $SO_3CF_3^-$, ReO_4^-) has been prepared [5,8–15]. All reported compounds exhibit a high-temperature spin crossover $^1A_1 \Leftrightarrow {}^5T_2$ and transition temperatures T_c are in the temperature range 310–470 K. Recently we described the synthesis of mononuclear Fe(II) complex of *tris*(pyrazol-1-yl)methane with *p*-sulfonatothiacalix[4]arene ($TC[4]AS^{4-}$): $[Fe\{HC(pz)_3\}_2]_2(TC[4]AS)$ [14]. The outer sphere inclusion of cation into thiacalix[4]arene cavity was established only by ^{1}H NMR spectroscopy in aqueous solution. The complex exhibits high temperature spin crossover without hysteresis on $\mu_{eff}(T)$ dependence. The SCO in the compound is accompanied by the thermochromism. The SCO temperature (T_c) for this complex is equal to 450 K. The T_c value was determined as the inflection point of the $\mu_{eff}(T)$ curve localized by the zero second derivative $\partial^2\mu_{eff}/\partial T^2$ because in the high temperature region $\mu_{eff}(T)$ curve does not reach the plateau due to the Fe(II) oxidation.

It was found that inclusion of $[Fe\{HC(pz)_3\}_2]^{2+}$ into the *p*-sulfonatothiacalix[4]arene cavity lead to a less abrupt transition $^1A_1 \Leftrightarrow {}^5T_2$ and an increase of SCO temperature by 10 K in comparison with $[Fe\{HC(pz)_3\}_2](ns)_2$ [16], where ns = 2-naphthalenesulfonate $C_{10}H_7SO_3^-$. At the same time, the cation inclusion into the macrocycle cavity increase the thermal stability by 20° (from 460

* Corresponding author.
E-mail address: svsol@iopc.ru (S. Solovieva).

https://doi.org/10.1016/j.ica.2018.02.021
0020-1693/

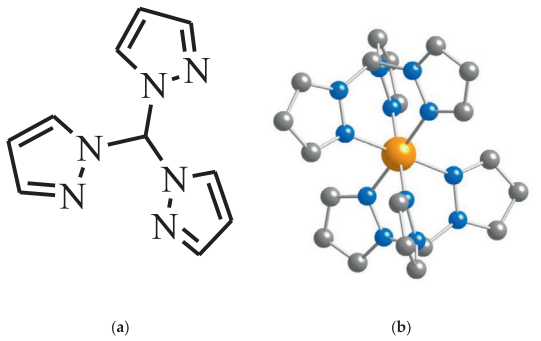

(a) (b)

Scheme 1. Molecular structure of $HC(pz)_3$ ligand (a) and its $[Fe\{HC(pz)_3\}_2]^{2+}$ complex (b).

up to 480 K) compared to naphthalenesulfonate analogue. In our opinion, further study of inclusion compounds of iron(II) *tris*(pyrazol-1-yl)methane complex with calixarenes derivatives allows to estimate the effect of macrocycle supramolecular interactions on the SCO characteristics.

To establish the effect of cyclophane structure on magnetic properties (SCO) and thermal stability of Fe(II) tris(pyrazol-1-yl) methane complex with the *p*-sulfonatocalix[4]arene (C[4]AS) as outer sphere counterion was investigated. Well-known C[4]AS forms the stable inclusion complexes with positively charged metal containing cations [17–19]. Moreover, methylene bridged calixarenes are more thermodynamically stable than its thia-analogs because C—C bond (389 kJ mol^{-1} in Ph-CH3 [20]) is stronger than C—S (314 kJ mol^{-1} in Ph-SH) [21]). So, we expected the grows of thermal stability of C[4]AS inclusion compounds in comparison with earlier investigated TC[4]AS one [14].

In addition, it should be noted that H_4(C[4]AS) can be easily deprotonated in aqueous solution with the formation of tetra- (C[4]AS^{4-}) or even penta- (C[4]AS^{5-}) anions due to the dissociation of four —SO_3H groups located on the upper rim and one phenolic OH group (Scheme 2) [22,23]. This feature in combination with hydrophobic cavity makes this ligand particular attractive to form inclusion compounds with the positively charged metal complexes.

Herein we report the synthesis and crystal structure of inclusion compounds based on iron(II) *tris*(pyrazol-1-yl)methane complex with *p*-sulfonatocalix[4]arenes and the SCO properties for the dehydrated complex.

2. Experimental section

2.1. Materials and general methods

Commercially available $FeSO_4·7H_2O$ (Sigma) was purified by recrystallization from an acidified aqueous solution. Ascorbic acid (ICN Biomedical) and $Ba(NO_3)_2$ (Aldrich) were used without further purification. *Tris*(pyrizol-1-yl)methane and C[4]AS were synthesized according to literature procedures [10,24]. The C/H/N elemental analysis was performed using a EURO EA 3000 (EuroVector) analyzer.

The diffuse reflectance spectra (DRS) were recorded on UV-3101 PC Shimadzu scanning spectrophotometer at a room temperature. The thermal analysis curve of complex **I** was registered on STA 409 PC Luxx NETZSCH equipped with a silicon carbide furnace on air in aluminum crucibles at the heating rate of 10°/min.

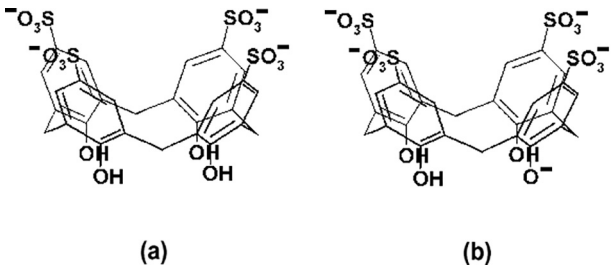

(a) (b)

Scheme 2. Tetra-anion CAS^{4-} (a) and penta-anion CAS^{5-} (b) of *p*-sulfonatocalixarene.

2.2. Synthesis of $[Fe\{HC(pz)_3\}_2]_5(C[4]AS)_2·16H_2O$ (*I*)

0.5 mmol (0.14 g) of $FeSO_4·7H_2O$ was dissolved in 3 ml of distilled water acidified by 0.05 g of ascorbic acid. A solution of $Ba(NO_3)_2$ (0.5 mmol, 0.13 g) in 5 ml of water was slowly added and barium sulfate was removed by filtration. 0.25 mmol (0.19 g) of H_4(C[4]AS) was dissolved in 3 ml of distilled water, alkalized with 1 mmol (0.056 g) of KOH. Then solution of K_4(C[4]AS^{4-}) was rapidly added to the mixture of *tris(*pyrazol-1-yl)methane (0.21 g, 1 mmol) and iron(II) nitrate in ethanol. A purple powder of *[Fe{HC(pz)$_3$}$_2$]$_5$(C[4]AS)$_2$·16H$_2$O* **I** was formed after stirring during 3 h. A precipitate was filtrated, washed with water and ethanol, dried on the air and finally over anhydrone in a desiccator. The yield of **I** is 45–50%. The elemental analysis data: for $C_{156}H_{170}Fe_5N_{60}O_{48}S_8$ (4189.2) calcd. C 44.6, H 4.3, N 20.0, Fe 6.7; for $[Fe\{HC(pz)_3\}_2]_5$(C[4]$AS)_2·16H_2O$ found C 42.5, H 4.1, N 21.3, Fe 6.6. The content of sixteen water molecules was determined by TGA method.

2.3. Synthesis of $[Fe\{HC(pz)_3\}_2]_2(C[4]AS)·24H_2O$ (*II*)

After filtration of the complex **I**, the mother liquor was left to crystallize at room temperature. Purple single crystals **II** suitable for SC-XDR were formed with very low yield in three weeks.

2.4. Synthesis of $[Fe\{HC(pz)_3\}_2]_5(C[4]AS)_2·62H_2O$ (*III*)

A small amount of **I** was dissolved in water and allowed to slowly evaporate at room temperature. Purple single crystals of **III** suitable for SC-XDR were formed during one week.

2.5. X-ray crystallography

X-ray diffraction data of **II**, **III** were obtained on a Bruker Nonius X8 Apex automated four-circle diffractometer equipped with a two-dimensional CCD-detector at 150(2) K (MoK_α-radiation, λ = 0.71073 Å, graphite monochromator). The single crystals have typical dimensions of 0.38 × 0.25 × 0.23 and 0.35 × 0.15 × 0.15 mm^3 for **II** and **III**, respectively. The reflection intensities were collected via ϕ and ω scanning within a narrow (0.5°) frames. The absorption corrections were applied empirically using a SADABS software package [25]. The structures were solved using a direct method and refined by means of full matrix least-squares in the anisotropic approximation for non-hydrogen atoms with the help of a SHELXTL software package [26]. Both structures were treated with [27] to extract highly disordered solvent electron density. There are four cavities in the unit cell of **II** with the volume of 1457 $Å^3$ and 531 *e* in the each cavity. It corresponds to 48–53 water molecules per cavity based on the volume of water molecule about 30 $Å^3$ as in the liquid water. In the case of **III** one cavity of 2028 $Å^3$ and 622 *e* per unit cell was determined that can be referred to 62–68 water molecules per crystal cell. The details of crystal data and selected bond lengths for compounds **II**, **III** are listed in Table 1 and Table S1. Crystallographic data were deposited with the following Cambridge Crystallographic Data Centre codes: CCDC 1,555,460 and 1,555,461 for **II**, **III**, respectively.

Table 1
Details of XRD experiment and crystallographic data for the complexes **II** and **III**.

Crystal	**II**	**III**
Molecular formula	$(C_{20}H_{20}FeN_{12})_2(C_{28}H_{20}O_{16}S_4)\cdot 24(H_2O)$	$(C_{20}H_{20}FeN_{12})(C_{20}H_{20}FeN_{12})_{2.5}\cdot 31(H_2O)$
Formula weight	1709.34	1950.45
Crystal system	Monoclinic	Triclinic
Space group	C 2/c	P-1
a, Å	44.745(3)	14.8368(3)
b, Å	16.110(1)	17.1718(6)
c, Å	31.611(2)	24.7632(8)
α, °	90	99.826(1)
β, °	124.063(2)	106.941(1)
γ, °	90	98.655(1)
V, Å^3	18878(2)	5811.0(3)
Z	8	2
Calc. density, g cm^{-3}	1.203	1.115
μ, mm^{-1}	0.463	0.444
Crystal size, mm^3	0.38 × 0.25 × 0.23	0.35 × 0.15 × 0.15
θ range, °	1.38–26.37	0.88–25.68
Index ranges	$-55 \le h \le 55$ $-20 \le k \le 19$ $-39 \le l \le 38$	$-17 \le h \le 10$ $-20 \le k \le 20$ $-30 \le l \le 30$
Reflections collected/independent (R_{int})	100283/19228 (0.0431)	39367/21543 (0.0199)
Completeness, %	99.6	97.6
Data/restraints/parameters	19228/0/1030	21543/16/1178
Goodness-of-fit	1.095	1.072
R_1, wR_2 ($I > 2\sigma(I)$)	0.0782, 0.1781	0.0613, 0.1784
R_1, wR_2 (all data)	0.0916, 0.1838	0.0816, 0.1923
$\Delta\rho_{max}$, $\Delta\rho_{min}$, eÅ^{-3}	1.139, −0.743	1.040, −0.736

2.6. Magnetic experiments

The static magnetic susceptibility of the polycrystalline sample was measured by Faraday method in the temperature range of 78–500 K at an external magnetic field strength amounting up to 5 kOe. The effective magnetic moment was calculated as $\mu_{eff} = (8\chi'_M T)^{1/2}$, where χ'_M is the molar magnetic susceptibility, corrected for diamagnetism. The heating (cooling) rate in the field of SCO was equal to 0.5 K/min.

3. Results and discussions

3.1. Synthesis and characterization of *I–III*

The synthesis of complexes was performed by mixing of water-ethanol solutions of $[Fe\{HC(pz)_3\}_2]^{2+}$ and aqueous solutions of K_4(C[4]AS). The solutions of iron salts were acidified by ascorbic acid to avoid Fe^{2+} oxidation ($pH = 4$). Generally, phenols are considered as weak acids. For example, pK_a of the *p*-hydroxybenzenesulfonate is equal to 8.9 [28], but the acidic properties are enhanced considerably in the case of *p*-sulfonatocalix[4]arene. This fact is explained by the stabilization of monodissociated species by two hydrogen bonds of one oxide anion with the adjacent phenolic hydroxyl groups [22]. This causes the remarkable shift of pK_{a1} down to 3.3 and the dissociation of the first proton occurs at relatively low pH values. Further acid dissociation is observed under basic conditions (pK_{a2}–pK_{a4} = 11.8–14) [20,21]. Thus, the ratio [C[4]AS^{5-}]/[C[4]AS^{4-}] under the synthetic conditions is equal to 5.5. It means that 85% of the anion is in the form of C[4]AS^{5-}. It plays one of the key roles in the interactions of $[Fe\{HC(pz)_3\}_2]^{2+}$ with calix[4]arenes in accordance with the equilibria:

$$5[Fe\{HC(pz)_3\}_2]^{2+} + 2C[4]AS^{5-} \leftrightarrows [Fe\{HC(pz)_3\}_2]_5(C[4]AS^{5-})_2$$

$$2[Fe\{HC(pz)_3\}_2]^{2+} + C[4]AS^{4-} \leftrightarrows [Fe\{HC(pz)_3\}_2]_2(C[4]AS^{4-})$$

The elemental analysis of **I–III** revealed the formed compounds to be hydrates. The complexes are soluble in water, ethanol, isopropanol, acetone and CH_2Cl_2 and insoluble in benzene and toluene. They are stable in air at a room temperature for a long time.

The possible pattern of the inclusion complex between *p*-sulfonatocalix[4]arene and positive charged guest according to the literature data [17–19] is as follows: the complex cation $[Fe\{HC(pz)_3\}_2]^{2+}$ is partially incorporated into macrocycle cavity with 1:1 host-guest stoichiometry. The stabilization of such type complexes is ensured by strong electrostatic interactions between the positively charged cation and the negatively charged sulphonato groups as well as weak CH-π and π–π interactions. To establish a crystal structure of obtained Fe(II) complexes the X-ray analysis on single crystal has been performed. It revealed the formation of two complexes in crystalline phase with the following formula $[Fe\{HC(pz)_3\}_2]_2(C[4]AS^{4-})\cdot 24H_2O$ (**II**) and $[Fe\{HC(pz)_3\}_2]_5(C[4]AS^{5-})_2\cdot 62H_2O$ (**III**). In both cases 1:1 host-guest inclusion complexes were observed (Fig. 1). The coordination sphere of Fe(II) cations in the crystal were found to be close to octahedral with 6 N atoms of pyrazolyl moieties belonging to two $HC(pz)_3$ ligands (d_{Fe-N} = 1.95–1.99 Å, see Table S1, Scheme 1).

It should be noted that such type of coordination environment corresponds to low-spin states of Fe(II) cations and is quite similar to those $[Fe\{HC(pz)_3\}_2]A_2$ complexes previously reported (A = Cl^-, Br^-, I^-, SiF_6^{2-}, $SO_3CF_3^-$, ReO_4^-) and $[Fe\{HC(pz)_3\}_2]SO_4$ [10–12]. All four sulfonato-groups were found to be deprotonated in both structures as well as one OH groups of the low rim of macrocycle in the case of **III** (Scheme 2). For **II** and **III**, one $[Fe\{HC(pz)_3\}_2]^{2+}$ complex cation is included into calix[4]arene cavity due to electrostatic and weak CH–π interactions ($d_{CH(pz)-C6centroid}$ = 3.751 Å and 3.722 Å, respectively), whereas other are located without any specific interaction with macrocycle within the crystal lattice. It should be mentioned also that in both structures the inclusion phenomena leads to a slight distortion of geometry of calix[4]arene molecules which adopt a *pinched cone* conformation according to

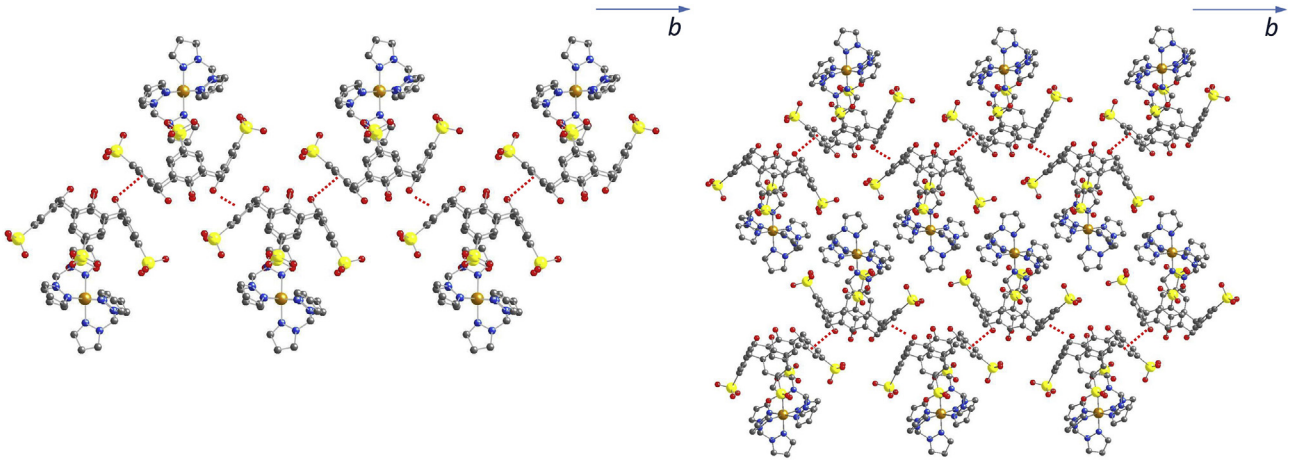

Fig. 1. A portion of crystal structure of **II** showing the side by side arrangement of calix[4]arene inclusion complexes leading to 1D chains formation through OH π interactions along the *b* axis (a) and their antiparallel stacking in layers perpendicular to [0 1 0] plane (b). Grey, yellow, blue, red and goldish atoms represent C, S, N, O and Fe atoms, respectively. H atoms and solvent molecules are omitted for clarity. (For interpretation of the references to colour in this figure legend, the reader is referred to the web version of this article.)

Table 2
Dihedral angles between the opposite aryl units and S-S distances of distal situated SO_3^- groups for **II** and **III**.

	II	III
Dihedral angles (°)	128.22	125.02
	107.05	102.17
$d(S_{so3}\text{-}S_{so3})$ (Å)	10.85	11.02
	8.93	9.31

the dihedral angles between the opposite aryl units of calix[4]arene platform and S-S distances of distal situated SO_3^- groups (see Table 2).

Moreover, the depth of penetration of the aromatic moiety into the cavity may be measured by the distance of the centroid of the included pyrazolyl ring from the plane fitted through four CH_2 bridging moieties. For **II** and **III**, this parameter is equal to 4.364 and 4.405 Å, respectively, which corresponds to the values observed for previously described *p*-sulfonatocalix[4]arene based inclusion compounds [29]. Another comparison concerns the angle made by the plane of the aromatic guest with the plane of the CH_2 carbon atoms that was found close to be perpendicular (85.05° for **II** and 81.39° for **III**) and caused by enhanced hydrophobic interaction of calixarene cavity with included pyrazolyl moiety.

The structures of **II** and **III** in the crystalline phase present different supramolecular motifs. In crystal of **II**, the inclusion complexes of *p*-sulfonatocalix[4]arene are arranged in alternate fashion leading to 1D supramolecular chains formation along the *b* axis provided by week OH–π interaction between one phenolic hydroxyl group and one aryl unit of adjacent calixarene molecules (3.089 Å) (Fig. 1a). Within the crystal, these negative charged chains are stacked in antiparallel mode along *b* axis and form the antiparallel layers perpendicular to [0 1 0] crystallographic plane (Fig. 1b). The 3D crystal packing is completed by stacking of latest ones along *c* axis through the electrostatic interaction with remained $[Fe\{HC(pz)_3\}_2]^{2+}$ cationic species leading to neural crystal structure containing pores filled by water molecules (Fig. 2).

In the case of **III**, the deprotonation of one calix[4]arene OH phenolic group significantly change the supramolecular motif of complexes in crystalline phase. In crystal of **III**, they are arranged in alternate fashion respecting to an axis without any specific

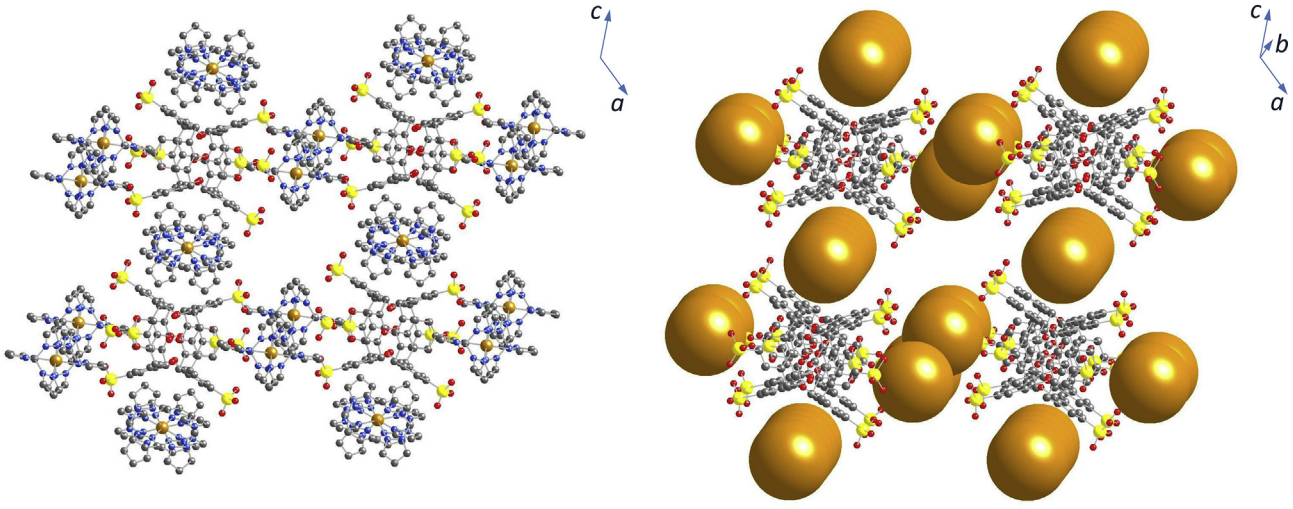

Fig. 2. A 3D crystal packing of **II** (b) and its schematic representation (b). Grey, yellow, blue, red and goldish atoms represent C, S, N, O and Fe atoms, respectively. H atoms and solvent molecules are omitted for clarity. (For interpretation of the references to colour in this figure legend, the reader is referred to the web version of this article.)

contacts between them leading to 2D negative charged layers formation along the *ac* plane (Fig. 3a). The un-included complex Fe(II) cations are lying in the interstices between the calixarene based inclusion complexes by decreasing their negative charge from −3 till −1 (Fig. 3b). Finally, the neutralization of overall 3D crystal structure is achieved by the connection of negative charged layers with remained $[Fe\{HC(pz)_3\}_2]^{2+}$ cationic species through electrostatic interaction along *b* axis (Fig. 4). Because of a large size of complex Fe(II) cations, like in the case of **II**, the 3D crystal arrangement of **III** also affords to cavities formation along *c* crystallographic axis which are filled by the H_2O molecules. One sulphur atom of four SO_3^- groups of calix[4]arene in **III** is found to be disordered.

Unfortunately, we couldn't study crystal structures of high-spin form of obtained complexes because of their low stability under X-ray experiment conditions (only ~20 min under the effect of high-energy radiation at room temperature).

4. Spectral experiments

According to the IR spectroscopic data for the complex $[Fe\{HC(pz)_3\}_2]_5(C[4]AS)_2\cdot 16H_2O$ (**I**), the most significant changes are observed in the region of 850–860 cm^{-1} and 980–1000 cm^{-1} (Fig. 5). The temperature rise up to 160 °C leads to the intensity increase of bands at 853 and 980 cm^{-1} and decrease at 866 and 990 cm^{-1}. The intensities of the bands at 1452 and 1412 cm^{-1} are decreased with the temperature growth. The same temperature regularities in IR spectra were also found for a number of $[Fe\{HC(pz)_3\}_2]^{2+}$ complexes with other counterions [5,8–15].

The IR absorption of pyrazole rings is appeared in the range of 1600–1400 cm^{-1}. It is sensitive to the coordination of nitrogen atoms of the pyrazole rings with Fe(II) ion. That is why these bands are significantly shifted relatively ligand ones. Broad bands (3560–3400 cm^{-1}) corresponding to the stretching vibrations of O—H bonds of water are observed in high-frequency part of the

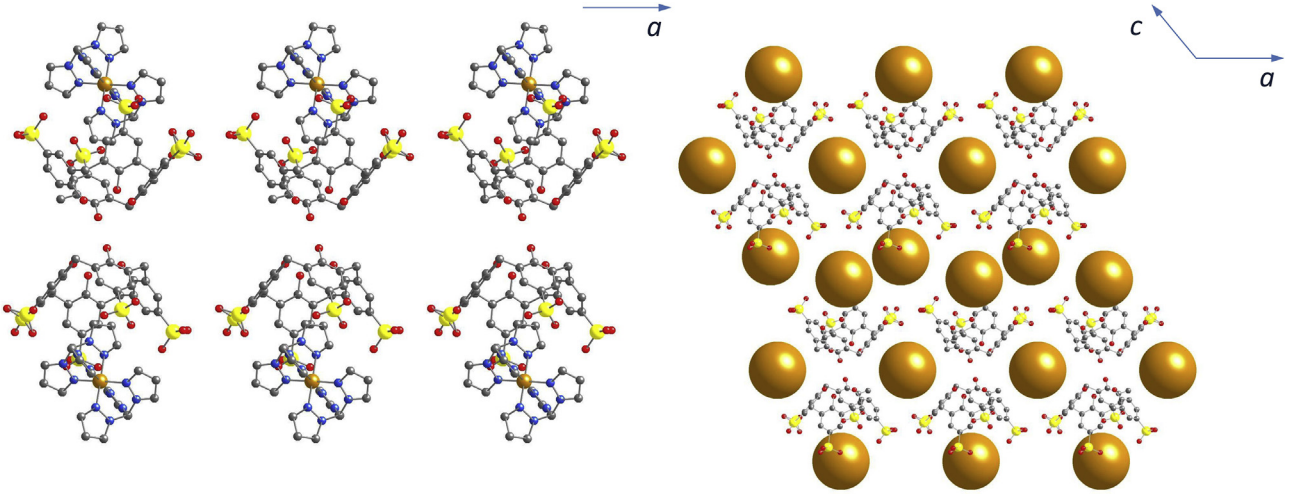

Fig. 3. A portion of crystal structure of **III** showing alternate arrangement of inclusion complexes based on *p*-sulfonatocalixarene molecules along *a* crystallographic axis (a), schematic representation of Fe(II)-calixarene based layer in the *ac* plane (b). Grey, yellow, blue, red and goldish atoms represent C, S, N, O and Fe atoms, respectively. Major goldish spheres represent complex $[Fe\{HC(pz)_3\}_2]^{2+}$ cations. H atoms and solvent molecules are omitted for clarity. (For interpretation of the references to colour in this figure legend, the reader is referred to the web version of this article.)

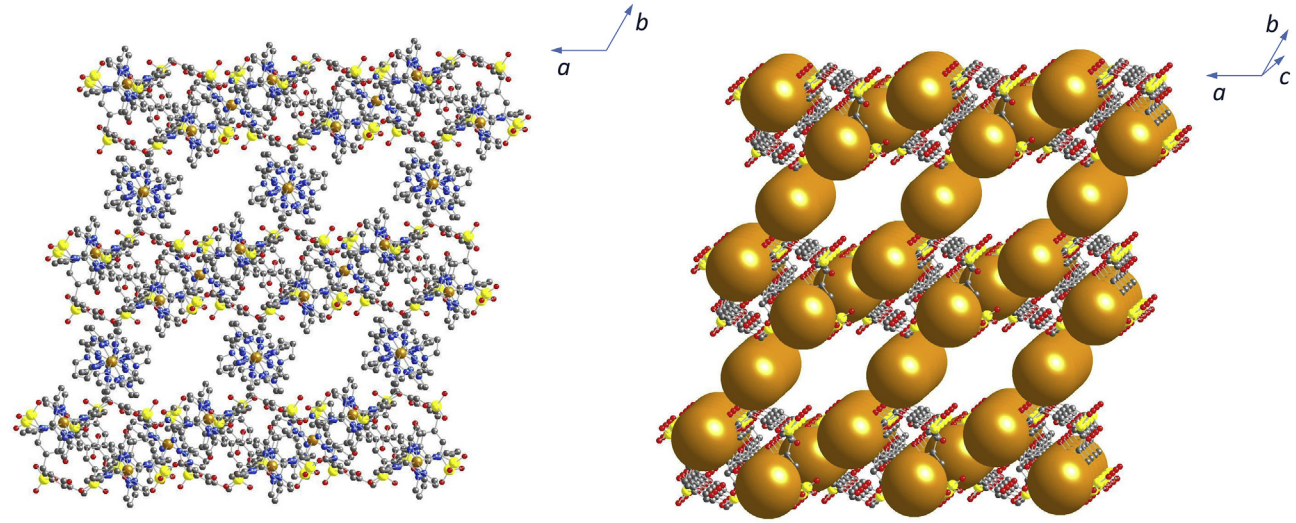

Fig. 4. A 3D crystal packing of **III** (a) and its schematic representation (b). Grey, yellow, blue, red and goldish atoms represent C, S, N, O and Fe atoms, respectively. Major goldish spheres represent complex $[Fe\{HC(pz)_3\}_2]^{2+}$ cations. H atoms and solvent molecules are omitted for clarity. (For interpretation of the references to colour in this figure legend, the reader is referred to the web version of this article.)

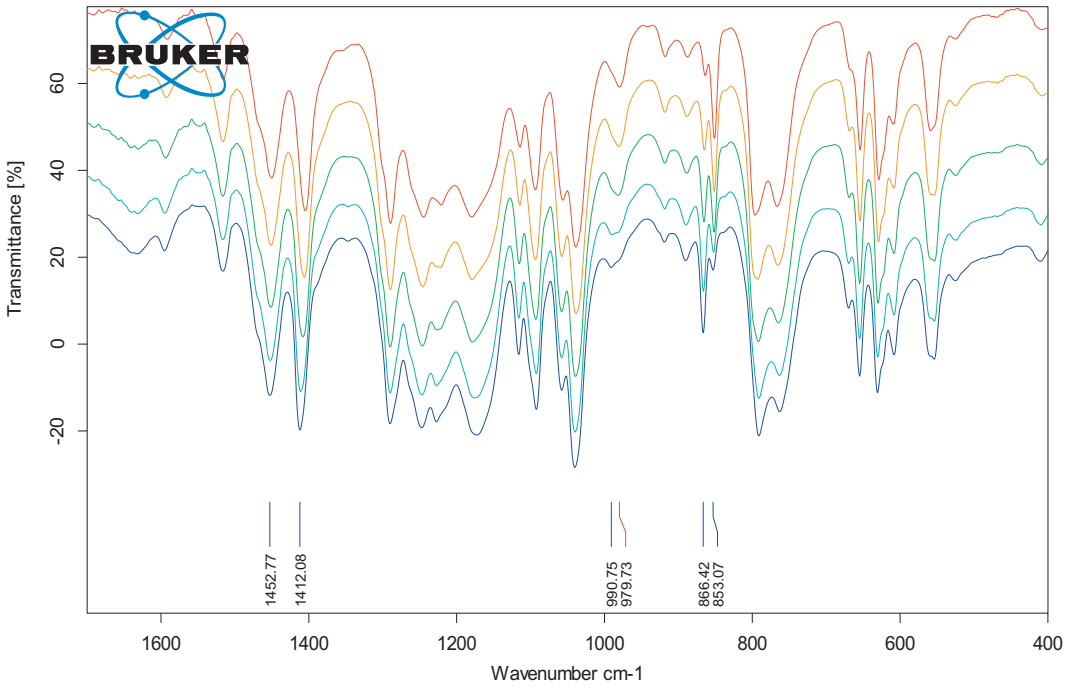

Fig. 5. The IR spectra of $[Fe\{HC(pz)_3\}_2]_5(CAS)_2{\cdot}16H_2O$ (**I**) as a function of temperature (from the bottom upwards 25, 50, 90, 120, 160 °C).

spectrum. Absorption bands of C[4]AS are characterise for calix[4] arene platform [30–32].

The UV–Vis diffuse reflection spectrum (DRS) of powder complex **I** at the room temperature shows a broad band in the range of 450–600 nm with λ_{max} at 523 nm (Fig. S2) that could be assigned to $^1A_1 \rightarrow {}^1T_1$ *d–d* transition in a strong ligand field of distorted O_h symmetry inherent in the cation. The strength of the ligand field (parameter Δ_{LS}, cm^{-1}) of *tris*(pyrazol-1-yl)methane can be estimated. For complex **I** it is equal to 20130 cm^{-1}. Earlier it was established the region of Δ_{LS} values that cause the SCO appearance: 19000 $cm^{-1} \leq \Delta_{HC} \leq 23000$ cm^{-1} [33]. Thus, this condition is satisfied for complex **I** and SCO properties can be expected.

5. Thermal analysis

The thermal stability of $[Fe\{HC(pz)_3\}_2]_5(C[4]AS)_2{\cdot}16H_2O$ (**I**) was studied by the thermogravimetric analysis (TGA) technique. At the temperature range 320–390 K, compound exhibits the weight loss of water molecules, which is about 6.9% (Fig. S4) and corresponds to the loss of sixteen water molecules (calcd. 6.88%). Then, the structural framework starts to collapse at about 500 K. Finally, the decomposition residue was assumed to be the iron oxides mixture.

6. Magnetic measurements

For magnetic measurements the polycrystalline sample was pre-dehydrated to a constant weight. The magnetochemical investigation was carried out with the dehydrated complex, $[Fe\{HC(pz)_3\}_2]_5(C[4]AS)_2$, within the temperature range of 78–500 K. It is evident that the inclusion of $[Fe\{HC(pz)_3\}_2]^{2+}$ into the *p*-sulfonatocalix[4]arene cavity results in increasing of the thermal stability of iron(II) complex. It is shown that the complex exhibits a high-temperature $^1A_1 \Leftrightarrow {}^5T_2$ spin crossover, whereas the $\mu_{eff}(T)$ curve reaches 4.56 B.M. (Fig. S3). The value of the effective magnetic moment μ_{eff} = 1.09 B.M. at 80 K is in a good agreement with Van

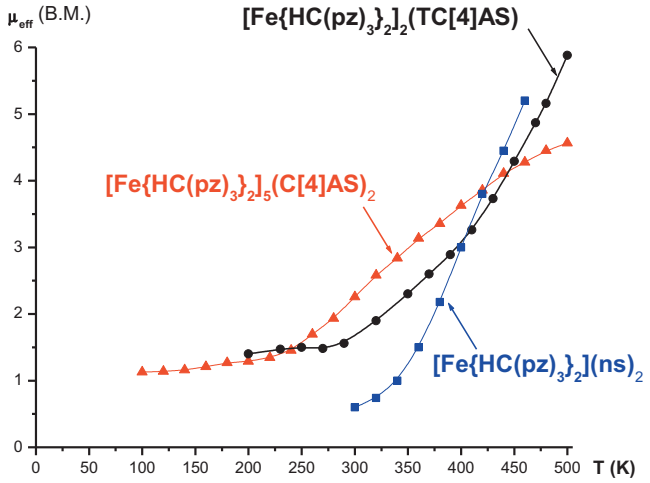

Fig. 6. The $\mu_{eff}(T)$ plots for $[Fe\{HC(pz)_3\}_2]_5(CAS)_2$, $[Fe\{HC(pz)_3\}_2]_2(TCAS)$ [14] and $[Fe\{HC(pz)_3\}_2](ns)_2$ [16].

Fig. 7. The thermochromism of crystal $[Fe\{HC(pz)_3\}_2]_5(CAS)_2{\cdot}62H_2O$ (**III**).

Vleck's temperature independent paramagnetism. The crossover temperature T_c for heating and cooling are equal to 390 K and 380 K, respectively.

It is necessary to note that T_c of $[Fe\{HC(pz)_3\}_2]_5(C[4]AS)_2$ is significantly decreased by 60 K in comparison with thia-analog $[Fe\{HC(pz)_3\}_2]_2(TC[4]AS)$. Compared to $[Fe\{HC(pz)_3\}_2]_2(TC[4]AS)$ and $[Fe\{HC(pz)_3\}_2](ns)_2$ the complex $[Fe\{HC(pz)_3\}_2]_5(C[4]AS)_2$ is more stable in the high temperature region (at ~500 K) and $\mu_{eff}(T)$ curve almost reaches a plateau (Fig. 6). The spin transition is accompanied by thermochromism (Fig. 7) and the color of crystal is changed from purple to pink (not to white), that can be explained by the residual amounts of the LS state species in the sample after completing of the **SCO** process.

7. Conclusions

We prepared and characterized the spin-crossover compounds based on Fe(II) *tris*(pyrazol-1-yl)methane complex with *p*-sulfonatocalix[4]arene as outer sphere counterion of formula $[Fe\{HC(pz)_3\}_2]_5(C[4]AS)_2{\cdot}nH_2O$ ($n = 0$, 16, 62). The complexes exhibit high-temperature SCO $^1A_1 \Leftrightarrow {}^5T_2$ which is accompanied by thermochromism. The XRD data prove the inclusion of $[Fe\{HC(pz)_3\}_2]^{2+}$ into the cavity of *p*-sulfonatocalix[4]arene. The formation of inclusion complex of Fe(II) *tris*(pyrazol-1-yl)methane complex with *p*-sulfonatocalix[4]arene leads to thermal stabilization and decreasing of **SCO** temperature. So, the supramolecular interactions allow to tune the SCO properties that is very important for molecular sensors applications. Further investigations of Fe(II) complexes based on calixarene platform are in progress.

Acknowledgments

The authors thank the Russian Foundation for Basic Research (project no 16-53-00020 Bel_a and 16-03-00920_a) for financial support. The authors express gratitude to I.V. Yushina (Nikolaev Institute of Inorganic Chemistry, Russia) for the DRS registration.

Appendix A. Supplementary data

Supplementary data associated with this article can be found, in the online version, at https://doi.org/10.1016/j.ica.2018.02.021.

References

[1] P. Gütlich, H. Goodwin, Spin Crossover in Transition Metal Compounds I–III, Topic in Curr. Chem., Springer-Verlag, Berlin, 2004, pp. 233–235.
[2] M.A. Halcrow, Spin-Crossover Materials Properties and Applications, J. Wiley & Sons Ltd., Chichester, UK, 2013.
[3] M. Shatruk, H. Phan, B.A. Chrisostomo, A. Suleimenova, Coord. Chem. Rev. 289 (2015) 62–73.
[4] S. Brooker, Chem. Soc. Rev. 44 (2015) 2880–2892.
[5] L.G. Lavrenova, O.G. Shakirova, Eur. J. Inorg. Chem. 5–6 (2013) 670–682.
[6] O. Kahn, J. Kröber, C. Jay, Adv. Mater. 4 (1992) 718–728.
[7] P. Gamez, J.S. Costa, M. Quesada, G. Aromi, J. Chem. Soc. Dalton Trans. (2009) 7845–7853.
[8] T. Astley, J.M. Gulbis, M.A. Hitchman, E.R.T. Tiekink, J. Chem. Soc. Dalton Trans. (1993) 509–515.
[9] P.A. Anderson, T. Astley, M.A. Hitchman, F.R. Keene, B. Moubaraki, K.S. Murray, B.W. Skelton, E.R.T. Tiekink, H. Toftlund, A.H. White, J. Chem. Soc. Dalton Trans. (2000) 3505–3512.
[10] D.L. Reger, C.A. Little, A.L. Rheingold, M. Lam, L.M. Liable-Sands, B. Rhagitan, T. Concolino, A. Mohan, G.J. Long, V. Briois, Inorg. Chem. 40 (2001) 1508–1520.
[11] L.D. Field, B.A. Messerle, L.P. Soler, T.W. Hambley, P. Turner, J. Organomet. Chem. 655 (2002) 146–157.
[12] G.J. Long, F. Grandjean, D.L. Reger, Top. Curr. Chem. 233 (2004) 91–122.
[13] O.G. Shakirova, L.G. Lavrenova, N.V. Kuratieva, D.Yu. Naumov, V.A. Daletskii, L. A. Sheludyakova, V.A. Logvinenko, S.F. Vasilevskii, Russ. J. Coord. Chem. 36 (2010) 275–283.
[14] O.G. Shakirova, L.G. Lavrenova, V.A. Daletsky, E.A. Shusharina, T.P. Griaznova, S. A. Katsyuba, V.V. Syakaev, V.V. Skripacheva, A.R. Mustafina, S.E. Soloveva, Inorg. Chim. Acta 363 (2010) 4059–4064.
[15] O.G. Shakirova, V.A. Daletsky, L.G. Lavrenova, N.V. Kuratieva, E.A. Shusharina, L. A. Sheludyakova, S.F. Vasilevskii, Russ. J. Coord. Chem. 37 (2011) 511–516.
[16] O.G. Shakirova, N.V. Kuratieva, E.V. Korotaev, L.G. Lavrenova, Solid State Phenom. 233–234 (2015) 534–537.
[17] A.R. Mustafina, V.V. Skripacheva, A.I. Konovalov, Russ. Chem. Rev. 76 (2007) 917–930.
[18] V.V. Skripacheva, A.R. Mustafina, N.V. Rusakova, V.V. Yanilkin, N.V. Nastapova, R.R. Amirov, V.A. Burilov, R.R. Zairov, S.S. Kost, S.E. Solovieva, Yu.V. Korovin, I.S. Antipin, A.I. Konovalov, Eur. J. Inorg. Chem. (2008) 3957–3963.
[19] A.R. Mustafina, V.V. Skripacheva, V.A. Burilov, V.V. Yanilkin, R.R. Amirov, A.S. Stepanov, S.E. Soloveva, I.S. Antipin, A.I. Konovalov, Inorg. Chim. Acta 362 (2009) 3279–3284.
[20] S.W. Benson, J. Chem. Educ. 42 (1965) 502–518.
[21] J.A. Kerr, Chem. Rev. 66 (1966) 465–500.
[22] S. Shinkai, Tetrahedron 49 (1993) 8933–8968.
[23] H. Matsumiya, Y. Terazono, N. Iki, S. Miyano, J. Chem. Soc. Perkin Trans. 2 (2002) 1166–1172.
[24] J.P. Scharff, M. Mahjoubi, New J. Chem. 15 (1991) 883–887.
[25] Bruker AXS Inc., APEX2 (Version 1.08), SAINT (Version 7.03), SADABS (Version 2.11), Bruker Advanced X-ray Solutions, Madison, WI, USA, 2004.
[26] G.M. Sheldrick, Acta Crystallogr. A 64 (2008) 112–122.
[27] A.L. Spek, Acta Crystallogr. C 71 (2015) 9–18.
[28] I. Yoshida, N. Yamamoto, F. Sagara, D. Ishii, K. Ueno, S. Shinkai, Bull. Chem. Soc. Jpn. 65 (1992) 1012–1015.
[29] J.L. Atwood, G.W. Orr, F. Hamada, R.L. Vincent, S.G. Bott, K.D. Robinson, J. Am. Chem. Soc. 113 (1991) 2760–2761.
[30] V.I. Kovalenko, A.V. Chernova, E.I. Borisoglebskaya, S.A. Katsyuba, V.V. Zverev, R.R. Shagidullin, I.S. Antipin, S.E. Solov'eva, I.I. Stoikov, A.I. Konovalov, Russ. Chem. Bull. 51 (2002) 825–827.
[31] V.L. Furer, E.I. Borisoglebskaya, V.I. Kovalenko, Spectrochim. Acta A 61 (2005) 355–359.
[32] S. Katsyuba, V. Kovalenko, A. Chernova, E. Vandyukova, V. Zverev, R. Shagidullin, I. Antipin, S. Solovieva, I. Stoikov, A. Konovalov, Org. Biomol. Chem. 3 (2005) 2558–2565.
[33] A. Hauser, Top. Curr. Chem. 233 (2004) 49–58.